Scaling properties of subgrid-scale energy dissipation

Sergei G. Chumakov*
Center for Nonlinear Studies, Los Alamos National Laboratory, Los Alamos NM 87544, USA
(Dated: To appear in Physics of Fluids in May 2007)

We use DNS of forced homogeneous isotropic turbulence with 256^3 and 512^3 grid points and Reynolds number based on Taylor microscale up to 250 to examine *a priori* the scaling properties of the subgrid-scale kinetic energy and its dissipation rate. It is found that the two quantities are strongly correlated and a power-law scaling assumption holds reasonably well. However, the scaling exponent, which was assumed to be weakly varying in previous studies, is found to change considerably with the filter characteristic width.

In the Large Eddy Simulation (LES), the large-scale features of the flow are resolved directly via numerical scheme while the effect of the unresolved scales of motion is accounted for by using subgrid-scale (SGS) models[1]. From the point of view of LES model development, the statistical information about behavior of the small-scale flow quantities is of great importance, for it can be used to verify the underlying assumptions of existing SGS models and provide constraints that have to be satisfied by the ones currently in development[2–5].

The governing equations for LES are obtained by applying a filtering procedure to the Navier-Stokes equations. In this study we consider the incompressible case:

$$\frac{\partial \bar{u}_i}{\partial x_i} = 0 \tag{1}$$

$$\frac{\partial \bar{u}_i}{\partial t} + \bar{u}_j \frac{\partial \bar{u}_i}{\partial x_j} = -\frac{\partial P}{\partial x_i} + \nu \frac{\partial^2 \bar{u}_i}{\partial x_j \partial x_j} - \frac{\partial \tau_{ij}}{\partial x_j}. \tag{2}$$

Here $\bar{u}_i = u_i * G$ is the filtered velocity, $P = p/\rho$ is the modified pressure, ν is the kinematic viscosity and $\tau_{ij} = \overline{u_i u_j} - \bar{u}_i \bar{u}_j$ is the SGS stress tensor, which has to be modeled. Summation over repeated indices is implied. The filter kernel G is assumed to be non-negative and satisfy $\|G\|_1 = 1$.

To solve the equations (1)-(2) numerically one needs to have a model for τ_{ij}. A sizable fraction of models for τ_{ij} in the current literature, referred to as one-equation models, employ the SGS kinetic energy $k_s = \tau_{ii}/2$ for modeling τ_{ij}: as a part of scalar eddy-viscosity[6–8], tensor eddy-viscosity[9] or a particular scaling factor[10–12]. To obtain k_s one needs to solve an auxiliary transport equation:

$$\frac{\partial k_s}{\partial t} + \bar{u}_i \frac{\partial k_s}{\partial x_i} = \Pi - \epsilon_s - \frac{\partial Q_i}{\partial x_i} + \nu \frac{\partial^2 k_s}{\partial x_i \partial x_i}. \tag{3}$$

Here $\Pi = -\tau_{ij}\bar{S}_{ij}$ is the term responsible for the energy transfer between resolved and subgrid scales (energy transfer term); $\bar{S}_{ij} = \frac{1}{2}(\partial \bar{u}_i/\partial x_j + \partial \bar{u}_j/\partial x_i)$ is the resolved strain-rate tensor; Q_i is the flux of k_s due to inertial and pressure terms, which is usually modeled using eddy-viscosity Ansatz, and ϵ_s is the dissipation rate of k_s given by

$$\epsilon_s = \nu \left[\overline{\frac{\partial u_i}{\partial x_j}\frac{\partial u_i}{\partial x_j}} - \frac{\partial \bar{u}_i}{\partial x_j}\frac{\partial \bar{u}_i}{\partial x_j} \right]. \tag{4}$$

The quality of models for τ_{ij} and ϵ_s is crucial for maintaining the correct energy budget in LES. While modeling τ_{ij} is responsible for the correct energy transfer between the resolved and subgrid scales and is ultimately responsible for the stability of LES calculations that employ zero-equation models, the model for ϵ_s plays the same role in LES calculations with one-equation models. Usually modeling of ϵ_s is dealt with by using

$$\epsilon_s \approx C_k \frac{k_s^{3/2}}{\Delta} \tag{5}$$

where Δ is the characteristic filter width (usually the size of the LES grid cell) and C_k is either given a fixed value $C_k = 1.0$ or determined dynamically[6–8,13]. This model relies on the assumption that for a fixed Δ, ϵ_s scales as $k_s^{3/2}$.

In general, the power-law scaling $\epsilon_s \sim k_s^\gamma$ has been indeed observed, e.g., in experimental measurements in atmospheric boundary layer[14] or in a hyperviscous turbulence simulation[15]. The former study reports the scaling exponent γ to be close to 1 while the latter claims that $\gamma = 2/3$ as a consequence of the fact that Kolmogorov Refined Similarity Hypothesis[16] holds not only for velocity differences, as originally formulated, but for other inertial range quantities as well. In another study[12] it was observed that $\gamma \approx 1/2$ gave the most plausible results in the *a priori* tests in terms of collapse of the probability density functions (PDFs) of the constant C_ϵ in the scale-similarity type model for ϵ_s:

$$\epsilon_s \approx C_\epsilon \left[\frac{2k_s}{L_{ii}}\right]^\gamma \nu \left[\widehat{\frac{\partial \bar{u}_i}{\partial x_j}\frac{\partial \bar{u}_i}{\partial x_j}} - \frac{\partial \hat{\bar{u}}_i}{\partial x_j}\frac{\partial \hat{\bar{u}}_i}{\partial x_j} \right]. \tag{6}$$

Here $L_{ij} = \widehat{\bar{u}_i \bar{u}_j} - \hat{\bar{u}}_i \hat{\bar{u}}_j$ is the Leonard term for τ_{ij} and $\widehat{(\cdot)}$ denotes the test-filtering operation.

The purpose of this Brief Communication is to conduct *a priori* testing of the assumption $\epsilon_s \sim k_s^\gamma$ using large-scale DNS of forced isotropic turbulence. The outcome of these tests provides us with the physical insight that can be used in model development for ϵ_s, which is believed to be of interest to both engineering and scientific LES communities.

The incompressible Navier-Stokes equations were solved in a periodic box with sides of length $L = 2\pi$ and

N grid points in every direction. A standard pseudo-spectral algorithm was used, fully de-aliased by a combination of spherical truncation and phase shifting[17,18]. The turbulence is sustained by a deterministic forcing term[19]. Two sets of data are used in this study: Set 1 with $N = 256$, $\nu = 1/900$ and Set 2 with $N = 512$, $\nu = 1/1800$.

The condition $k_{\max}\eta \geq 1.1$ was satisfied for all times to ensure that all important flow scales are resolved[20]. For Set 2, a stronger condition $k_{\max}\eta \geq 1.4$ was satisfied. Here $k_{\max} = N\sqrt{2}/3$ is the maximum significant wavenumber resolved by the grid, and η is the Kolmogorov length scale. The flow was initialized using velocity components with Gaussian distribution and random phases. Forcing was turned on and the flow was let to develop for approximately 10 turnover times, and after that the snapshots of the flow field were taken. The consecutive snapshots were separated by the time slightly larger than the eddy-turnover time so the data is assumed to be temporally uncorrelated. The average Reynolds number based on Taylor microscale was $R_\lambda \approx 185$ for Set 1, and $R_\lambda \approx 250$ for Set 2. Set 1 contains 120 snapshots taken from three realizations with different random number seeds, and Set 2 contains 108 snapshots taken from four different realizations. To obtain resolved and SGS quantities, we used Gaussian filters with characteristic widths Δ logarithmically spaced from 0.074 to 3.0 ($\approx 7\eta \ldots 312\eta$) for Set 1 and from 0.04 to 3.0 ($\approx 7\eta \ldots 526\eta$) for Set 2.

First we show that the SGS dissipation ϵ_s plays an important role in the energy budget. To demonstrate this we plot in the Fig. 1 the value of $\langle \epsilon_s / \overline{\epsilon'} \rangle$ vs. the SGS Reynolds number defined as $R_\Delta = \sqrt{k_s}\Delta/\nu$. Here, $\epsilon' = \nu(\partial u_i/\partial x_j)(\partial u_i/\partial x_j)$ is the pseudo-dissipation, the angular brackets denote the averaging across the entire domain and over the snapshots. It can be seen that $\langle \epsilon_s / \overline{\epsilon'} \rangle$ exhibits logarithmic dependence on R_Δ for small R_Δ (approximately $R_\Delta < 100$) and for $R_\Delta > 200$ the SGS dissipation contributes more than 90% to the total energy dissipation. Thus ϵ_s plays a crucial role in overall energy budget.

Let us denote $a = (\ln k_s - \langle \ln k_s \rangle)/\sigma_k$ and $b = (\ln \epsilon_s - \langle \ln \epsilon_s \rangle)/\sigma_k$, where σ_k^2 is the variance of $(\ln k_s)$. Angular brackets denote averaging over entire domain. In our simulations, the probability density function (PDF) of k_s appears to be very close to log-normal and thus a is very close to being a standard normal random variable. By plotting the conditional average $\langle b|a \rangle$, averaged over all snapshots, we can recover γ in $\epsilon_s \sim k_s^\gamma$ as the slope of the graph.

We begin by plotting $\langle b|a \rangle$ for both sets of data in the Fig. 2. On each panel, each curve corresponds to a filter of different characteristic width Δ, ordered in ascending order. Each subsequent curve is shifted by 0.25 up to facilitate comparison.

It is evident that for all considered filter sizes, ϵ_s and k_s appear to be strongly correlated and the conjecture $\epsilon_s \sim k_s^\gamma$ holds reasonably well. For Δ comparable to the

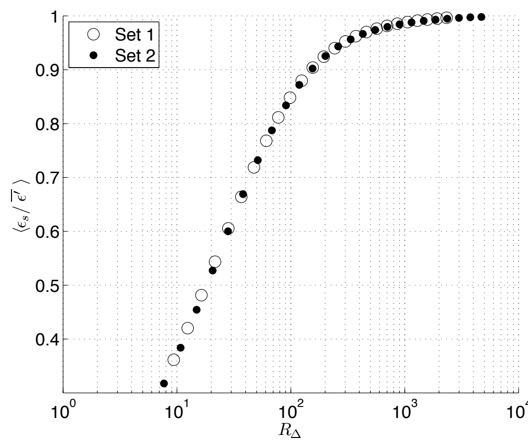

FIG. 1: Fraction of the dissipation represented by ϵ_s. Dependence on the SGS Reynolds number.

Kolmogorov length scale η (lower lines in the Fig. 2), the scaling exponent γ is close to 1. This filter size falls outside of the range reported in previous studies[14,15], the scaling can be understood using the following argument. For Δ close to η, using Leonard expansion[21], we can argue that

$$\epsilon_s \sim \Delta^2 \frac{\partial^2 \bar{u}_i}{\partial x_j \partial x_k} \frac{\partial^2 \bar{u}_i}{\partial x_j \partial x_k} \sim \Delta^2 \frac{(\delta u)^2}{\Delta^2} \frac{(\delta u)^2}{\Delta^2} \sim \Delta^2,$$

because the Taylor series approximation for δu for Δ/η close to 0 gives $\delta u \sim \Delta$. On the other hand, $k_s = \tau_{ii}/2$, and $\tau(\Delta) \sim (\delta u)^2$, as analytically shown by Eyink[22]. Here τ is the magnitude of τ_{ij} and δu is the magnitude of the velocity increment over the separation length Δ. Thus both k_s and ϵ_s scale as $(\delta u)^2$ for Δ in the near-viscous scale range.

For larger Δ, the scaling $\epsilon_s \sim k_s^\gamma$ still appears to hold reasonably well for the bulk of data (the area $|a| < 2$ corresponds to about 95% of the data). The slopes of the graphs diminish as Δ grows but there is no indication of any preferred value of γ. We plot the slopes extracted from both sets of data in the Fig. 3; error bars denote the variance of γ for each value of Δ. The slopes span the range between approximately 1/2 and 1 without noticeable plateau in the inertial range.

It should be noted that the curves in the Fig. 2 are systematically concave downward with the exception of the lowest curve in both panels. This indicates that a simple power law $\epsilon_s \sim k_s^\gamma$ does not hold exactly in the inertial subrange. However, taking into account the relatively narrow dispersion of data in the Fig. 3, it can be concluded that the power law provides an approximation to the correlation between ϵ_s and k_s that is reasonable enough to be used successfully in SGS modeling.

When plotted against the SGS Reynolds number R_Δ, the slopes from different datasets do not collapse to a single curve (not shown). However, when plotted against the filter width Δ as in Fig. 4, the mean values of γ almost coincide for two sets of data. This, in our opinion,

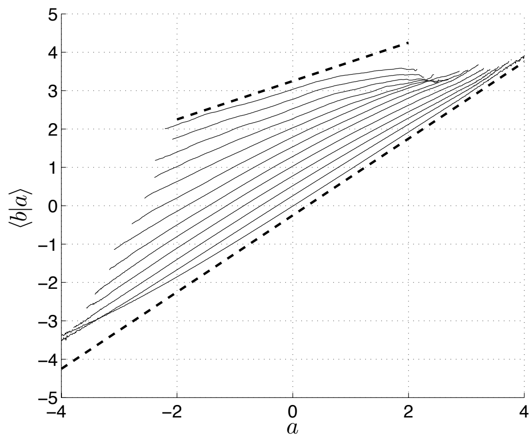

(a) Set 1

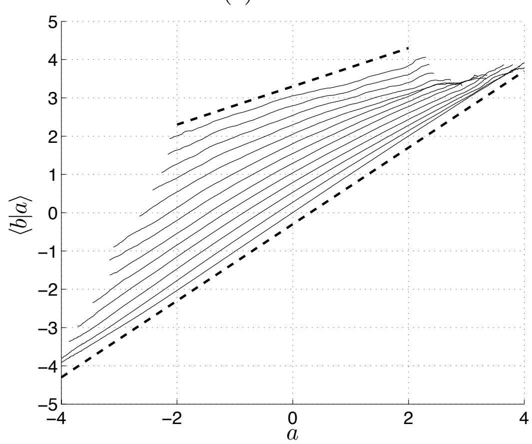

(b) Set 2

FIG. 2: The conditional averages $\langle b|a\rangle$. The dashed lines have the slopes of 1 (lower) and 1/2 (upper). The solid curves correspond to different filter width Δ, each subsequent curve is shifted up by 0.25 to facilitate comparison.

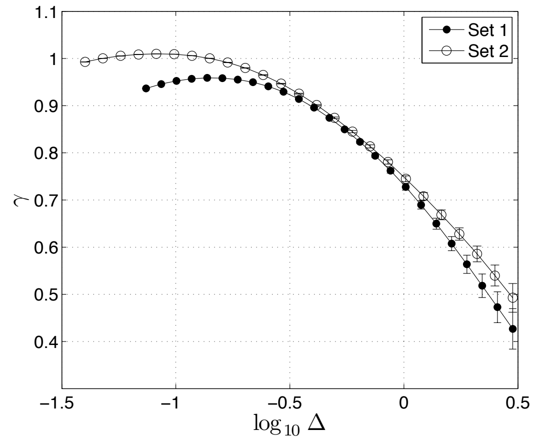

FIG. 3: Dependance of the average slope of $\langle b|a\rangle$ on the filter width Δ. Error bars give the variance of the data.

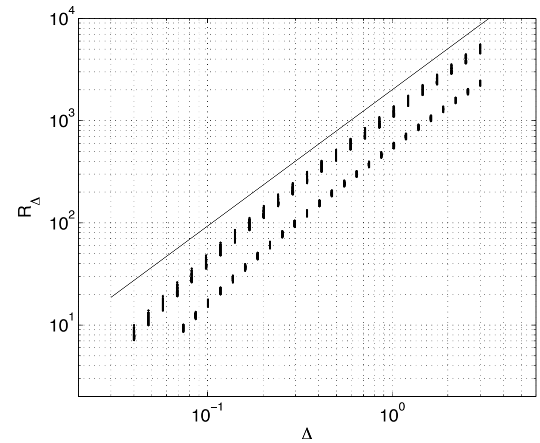

FIG. 4: Scaling of SGS Reynolds number R_Δ with Δ. Lower points correspond to the Set 1, higher points correspond to the Set 2. The solid line represents the scaling $\Delta^{4/3}$.

indicates that γ might depend more on the ratio of Δ to the lengthscale of forcing than on the SGS Reynolds number. To illustrate the difference in R_Δ between the two datasets, we plot R_Δ vs. Δ in the Fig. 4. The classical scaling $R_\Delta \sim \Delta^{4/3}$ is observed[20]. The values of R_Δ for Set 2 are about twice as large as ones for Set 1. This is explained by the fact that the only difference between 256^3 and 512^3 simulations is the value of ν while everything else including magnitude of forcing is kept intact. Thus, according to our data, in the inertial range the values of γ change from 0.5 to 0.9, γ is close to 1 in the near-viscous scale range and γ appears to depend more on Δ than R_Δ.

In conclusion, we found through direct numerical simulations of forced isotropic turbulence that the scaling assumption $\epsilon_s \sim k_s^\gamma$ holds reasonably well for SGS Reynolds number R_Δ of up to 5000. However, the value of γ was not found to be constant, as was assumed in previous studies by various authors[11,14,15], but rather to depend on the proximity of the LES filter size Δ to the forcing lengthscale. None of the observed scalings are close to $\epsilon_s \sim k_s^{3/2}$ which is widely used in the current literature. We found γ to be close to 1/2 for Δ close to forcing scale, which corresponds to results by Chumakov and Rutland[12]; for Δ in the near-viscous range the value of γ is close to 1, in accordance with Meneveau and O'Neal[14]. In the inertial range for both data sets, γ varies between 0.6 and 0.9 monotonically with Δ. The data from hyperviscous simulations[15] falls in this range with $\gamma = 2/3$. It should be noted that we do not see a visible plateau at $\gamma \approx 2/3$, as would be expected based on Refined Similarity Hypothesis.

Computations were performed on FOD cluster at the Center for Nonlinear Studies at LANL. Coyote and QSC supercomputers at LANL were used via Institutional Computing grant. The author is thankful to C. Meneveau for useful discussions and to D. Livescu for a version of DNS code. The author is indebted to the anonymous reviewer for valuable suggestions. This work was performed under auspices of the US Department of Energy

(W-7405-ENG).

---

* Electronic address: `chumakov@lanl.gov`

[1] P. Sagaut, *Large Eddy Simulation for Incompressible Flows: An Introduction.* Springer-Verlag, 2006.

[2] S. Cerutti and C. Meneveau, "Intermittency and relative scaling of subgrid-scale energy dissipation in isotropic turbulence," *Phys. Fluids*, vol. 10, no. 4, pp. 928–937, 1998.

[3] B. Tao, J. Katz, and C. Meneveau, "Statistical geometry of subgrid-scale stresses determined from holographic particle image velocimetry measurements," *J, Fluid Mech.*, vol. 547, pp. 35–78, 2002.

[4] H. S. Kang and C. Meneveau, "Effect of large-scale coherent structures on subgrid-scale stress and strain-rate eigenvector alignments in turbulent shear flow.," *Phys. Fluids*, vol. 17, no. 5, p. 055103, 2005.

[5] S. G. Chumakov, "Statistics of subgrid-scale stress states in homogeneous isotropic turbulence," *J. Fluid Mech.*, vol. 562, pp. 405–414, 2006.

[6] S. Ghosal, T. S. Lund, P. Moin, and K. Akselvoll, "A dynamic localization model for large-eddy simulation of turbulent flows," *J. Fluid Mech.*, vol. 319, pp. 353–385, 1995.

[7] S. Menon, P. K. Yeung, and W. W. Kim, "Effect of subgrid models on the computed interscale energy transfer in isotropic turbulence.," *Computers & fluids*, vol. 25, no. 2, pp. 165 – 80, 1996.

[8] A. Yoshizawa and K. Horiuti, "Statistically-derived subgrid-scale kinetic energy model for the large-eddy simulation of turbulent flows.," *J. Phys. Soc. Jpn.*, vol. 54, no. 8, pp. 2834 – 9, 1985.

[9] D. I. Pullin, "A vortex-based model for the subgrid flux of a passive scalar," *Phys. Fluids*, vol. 12, no. 9, pp. 2311–2319, 2000.

[10] E. Pomraning and C. J. Rutland, "Dynamic one-equation nonviscosity large-eddy simulation model," *AIAA J.*, vol. 40, no. 4, pp. 689–701, 2002.

[11] S. G. Chumakov and C. J. Rutland, "Dynamic structure models for scalar flux and dissipation in large eddy simulation," *AIAA J.*, vol. 42, no. 6, pp. 1132–1139, 2004.

[12] S. G. Chumakov and C. J. Rutland, "Dynamic structure subgrid-scale models for large eddy simulation," *Int. J. Numer. Meth. Fluids*, vol. 47, pp. 911–923, 2005.

[13] U. Schumann, "Subgrid scale model for finite difference simulations of turbulent flows in plane channels and annuli.," *J. Comput. Phys.*, vol. 18, no. 4, pp. 376 – 404, 1975.

[14] C. Meneveau and J. O'Neil, "Scaling laws of the dissipation rate of turbulent subgrid-scale kinetic energy," *Phys. Rev. E*, vol. 49, no. 4, pp. 2866–2874, 1994.

[15] V. Borue and S. A. Orszag, "Kolmogorov's refined similarity hypothesis for hyperviscous turbulence," *Phys. Rev. E*, vol. 53, no. 1, pp. R21–R24, 1996.

[16] A. N. Kolmogorov, "A refinement of previous hypotheses concerning the local structure of turbulence in a viscous incompressible fluid at high Reynolds numbers," *J. Fluid Mech.*, vol. 13, pp. 82–85, 1962.

[17] R. S. Rogallo, "Numerical experiments in homogeneous turbulence," Technical Memorandum 81315, NASA, Sept. 1981.

[18] C. Canuto, M. Hussaini, A. Quarteroni, and T. Zang, *Spectral Methods in Fluid Dynamics.* Berlin, Germany: Springer, 1988.

[19] L. Machiels, "Predictability of small-scale motion in isotropic turbulence," *Phys. Rev. Lett.*, vol. 79, no. 18, pp. 3411–3414, 1997.

[20] S. B. Pope, *Turbulent flows.* Cambridge Univ. Press, 2000.

[21] A. Leonard, "Energy cascade in large-eddy simulations of turbulent fluid flows," *Adv. Geophys.*, vol. 18, pp. 237–248, 1974.

[22] G. L. Eyink, "Locality of turbulent cascades," *Physica D*, vol. 207, pp. 91–116, 2005.